

# Irreversible mesoscale fluctuations herald the emergence of dynamical phases

Thomas Suchanek,<sup>1</sup> Klaus Kroy,<sup>1</sup> and Sarah A. M. Loos<sup>2,\*</sup>

<sup>1</sup>*Institut für Theoretische Physik, Universität Leipzig, Postfach 100 920, D-04009 Leipzig, Germany*

<sup>2</sup>*DAMTP, Centre for Mathematical Sciences, University of Cambridge, Wilberforce Road, Cambridge CB3 0WA, United Kingdom*

(Dated: March 30, 2023)

We study fluctuating field models with spontaneously emerging dynamical phases. We consider two typical transition scenarios, oscillatory instabilities and exceptional-point transitions associated with parity-time symmetry breaking. An analytical investigation of the low-noise limit reveals an unbounded increase of the mesoscopic entropy production rate towards the transition. For an illustrative model of two nonreciprocally coupled Cahn-Hilliard fields, we find physical interpretations in terms of fluctuating active interface dynamics and a coupling of modes near the exceptional point.

After A. Einstein's paper on Brownian motion had appeared, he received a critical letter from C. Röntgen [1] who reiterated the historically widespread concern that such “motion from heat” would violate the second law. He failed to understand that Einstein had just made precise the centuries-old notion of heat being but a name for the incessant random motion of the molecular constituents of all macroscopic matter [2]. In fact, these thermal fluctuations are a manifestation of conservation, not production, of energy and entropy. However, this cornerstone of modern equilibrium statistical mechanics is lost far from equilibrium, where it becomes a central task to understand whether, when, and why mesoscopic fluctuations produce entropy. With regard to biological systems, this literally becomes a question of “life and death”.

A fundamental property of any thermal equilibrium is time-reversal symmetry. Its breaking, in turn, reveals a production of entropy and the presence of dissipative dynamics. Noteworthy, on the coarse-grained scale, however, only a part of the full entropy production is generally perceptible. A versatile metric to quantify time-reversal symmetry breaking (TRSB) is the log-ratio of probabilities for forward and backward paths [3, 4]. This so-called (informatic) entropy production rate  $\mathcal{S}$  and related measures have recently been studied for a variety of systems; from single or few particle models [3], over nonequilibrium field theories of active matter [5–9], to experimental studies on multiscale biological systems [10–12].

In this Letter, we take a different perspective and explore how TRSB mesoscale fluctuations in many-body systems inform us about incipient pattern formation. Specifically, we address the TRSB associated with the emergence of *dynamical* meso phases, such as persistent travelling or oscillating patterns [13–24]. Such states are special examples of dissipative structures maintained by permanent dissipative energy currents [25–28]. Their spontaneous emergence is an instructive example of how a hidden nonequilibrium condition and its entropy production may reveal themselves mesoscopically. For example, for the Brusselator model, it was recently shown that  $\mathcal{S}$  may

display a significant increase across the static–dynamic phase transitions to its oscillating phase [7].

In this Letter, we consider a broad class of nonequilibrium field models with conserved dynamics, and focus on two prototypical static–dynamic transition scenarios, the well-known oscillatory instabilities [26, 29] and transitions with exceptional points (EXP) [30]. As was described only recently, the latter scenario generically occurs in systems with nonreciprocal interactions between two particle species [30–35], i.e., interactions that violate the action-reaction principle.

For both scenarios, we show that in the static phases the approach towards the static–dynamic transition is accompanied by a surge in entropy production that scales like the susceptibility, so that it would diverge at the transition, in the zero-noise limit. Further, we discover general connections between the parity-time ( $\mathcal{PT}$ ) symmetry breaking that generically occurs at EXPs, on the one hand, and the emergence of irreversible, i.e., TRSB fluctuations, on the other hand. We illustrate our general findings with a model of two nonreciprocally coupled Cahn-Hilliard field equations [31–34].

*Field theory and symmetry breaking.*— We study hydrodynamic field models of scalar components  $\phi_i(\mathbf{r}, t)$ ,  $i = 1, \dots, n$  of the following structure

$$\partial_t \phi_i = -\nabla \cdot \mathbf{J}_i, \quad \mathbf{J}_i = -\nabla \mu_i + \sqrt{2\epsilon} \mathbf{\Lambda}_i, \quad (1)$$

where  $\mathbf{J}_i$  is the current of the field  $\phi_i$ . The noise term  $\sqrt{2\epsilon} \mathbf{\Lambda}_i$  is constructed such that, in the equilibrium case, where  $\mu_i = \delta \mathcal{F} / \delta \phi_i$  derives from a free energy  $\mathcal{F}[\phi]$ , the resulting statistical field theory would obey a fluctuation–dissipation relation [36], with  $\epsilon$  denoting the noise intensity. However, for the case of a nonequilibrium deterministic current  $\mathbf{J}_i^d \equiv -\nabla \mu_i$ , which is of interest here, the chemical potential  $\mu_i$  cannot be represented as a gradient force. We further assume that Eq. (1) is symmetric with respect to parity inversion,  $\mathcal{P} : \mathbf{r} \mapsto -\mathbf{r}$ , thereby excluding externally driven systems.

A first useful insight is that, by construction, the spontaneous emergence of phases with travelling patterns in a model of type (1) is always accompanied by

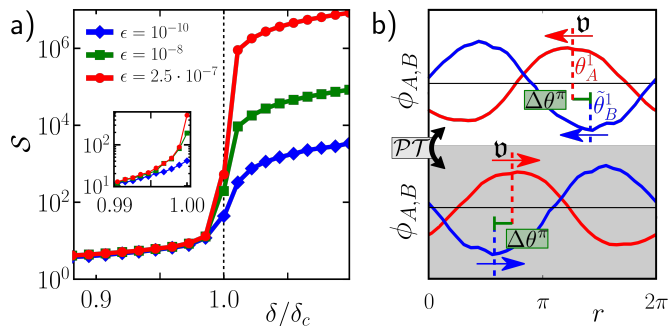


FIG. 1. Exceptional point (EXP) transition to a dynamical phase. (a) Entropy production rate near the transition point  $\delta_c$  from a static demixed to a travelling wave phase in model (6) ( $\alpha = -0.07, \gamma = 0.015, \kappa = 0.01, \beta = 0.05$ ) [40]. (b) Travelling wave solution of Eq. (6) and its image under a parity transformation  $\mathcal{P}$  (which yields another non-identical solution). The characteristic phase shift  $\Delta\theta^\pi$  is always aligned with the propagation velocity  $\mathbf{v}$  (indicated by arrows).

a breaking of  $\mathcal{PT}$  symmetry. This can be seen as follows. In a phase with travelling patterns, the zero-noise limit ( $\epsilon \rightarrow 0$ ) of Eq. (1) has solutions of the form  $\phi_i^*(\mathbf{r}, t) \equiv \varphi_i(\mathbf{r} - \mathbf{v}t)$ . Then, its  $\mathcal{P}$  invariance implies that  $\varphi'_i(\mathbf{r} + \mathbf{v}t)$ , with  $\varphi'_i(\mathbf{x}) = \mathcal{P}\varphi_i(\mathbf{x})$  is also a solution. Further,  $\varphi'_i(\mathbf{r} + \mathbf{v}t) = \mathcal{T}\varphi'_i(\mathbf{r} - \mathbf{v}t)$ , with  $\mathcal{T}$  the time-inversion operator. Therefore, the  $\mathcal{PT}$  operation applied to any given travelling pattern solution of Eq. (1) yields another solution. Now it is clear that, on the one hand, a parity symmetric pattern (i.e.,  $\varphi' = \varphi$ ) can occur only for  $\mathbf{v} = 0$ , and that, on the other hand, spontaneously emerging dynamical solutions  $\varphi$  with  $\mathbf{v} \neq 0$  automatically cease to be  $\mathcal{PT}$  eigenfunctions. Importantly, the emergence of  $\mathcal{PT}$  broken dynamical phases is not specific to field models of type (1) but observed in a much wider context, comprising polar swarm models [8, 30], directional solidification [37], or driven interfaces [38, 39].

*Irreversibility.*— To study irreversibility, we employ a framework [5, 6] that defines the entropy production  $s[\phi; 0, T]$  along a trajectory  $\{\phi_{t \in [0, T]}\}$  as the log ratio of forward and backward path probabilities (see Ref. [40] for details). The average rate of entropy production,  $\mathcal{S} = \lim_{h \rightarrow 0} \langle s[\phi; t, t+h]/h \rangle$ , serves as a measure of the breaking of detailed balance and of time-reversal symmetry at time  $t$ . Here,  $\langle \cdot \rangle$  denotes a formal ensemble average. A central result of Ref. [6] was that, in the steady state,  $\mathcal{S} = -\epsilon^{-1} \sum_i \int_V d\mathbf{r} \langle \dot{\phi}_i \mu_i \rangle$ , with  $V$  being the system's volume. From this, we derive another expression, which turns out to be particularly useful to study a transition to a dynamical state [40],

$$\mathcal{S} = \int_V d\mathbf{r} \frac{\sum_i \langle |\mathbf{J}_i^d|^2 \rangle}{\epsilon} + \int_V d\mathbf{r} \sum_i \left\langle \frac{\delta}{\delta\phi_i} \nabla \cdot \mathbf{J}_i^d \right\rangle \quad (2)$$

which is understood to be regularized by a UV-cut-off.

We consider the linear stability of the zero-noise solutions  $\phi^*$  of our dynamical system, i.e., the eigensystem of the Jacobian  $\mathcal{J}_{\phi^*}$  represented in a Fourier basis. A mode (eigenvector) becomes unstable when the real part of its eigenvalues vanishes. Due to the parity inversion invariance of Eq. (1),  $\mathcal{J}_{\phi^*}$  is real. We allow  $\mathcal{J}_{\phi^*}$  to be non-Hermitian, to capture a wide variety of nonequilibrium conditions [30, 41].

A common route from a (mesoscopically) static state to a dynamical state is via oscillatory instabilities. Such transitions are very similar to classical equilibrium critical transitions, except that they occur through a pair of complex conjugated eigenmodes of  $\mathcal{J}_{\phi^*}$  that become unstable and whose eigenvalues (here denoted by  $\lambda_\pm$ ) have non-vanishing imaginary parts. In contrast, the alternative scenario of EXP-transitions is not primarily characterized by the properties of the eigenvalues of  $\mathcal{J}_{\phi^*}$ , but by the fact that the modes that loose stability in the course of the transition become *collinear*. In the following, we assume that only two modes  $\hat{e}_0, \hat{e}_1$  are involved in the transition (whose eigenvalues we denote by  $\lambda_0$  and  $\lambda_1$ ) and that one of them is a *Goldstone* mode of a broken continuous symmetry, i.e.,  $\lambda_0 = 0$  for  $\hat{e}_0$ . In this case, the EXP-transition leads into a dynamical phase, which dynamically restores the continuous symmetry associated with this Goldstone mode [30].

Using Eq. (2), we deduce general characteristics of the entropy production rate  $\mathcal{S}$  in the vicinity of the transitions. Our first general finding is that for both above scenarios  $\mathcal{S}$  is of order  $\epsilon^0$ . Particularly informative is the behavior of the limit  $\mathcal{S}^* := \lim_{\epsilon \rightarrow 0} \mathcal{S}$ , which, although it may be not directly attainable itself, reveals the TRSB at *leading order* in  $\epsilon$ . For oscillatory instabilities of monochromatic modes of wavelength  $2\pi/|\mathbf{q}_j|$ ,  $\mathcal{S}^*$  behaves like

$$\mathcal{S}^* \sim |\mathbf{q}_j|^{-2} |\text{Im}\lambda_\pm|^2 \chi, \text{ as } \text{Re}\lambda_\pm \rightarrow 0, \quad (3)$$

where  $\chi \equiv \lim_{\epsilon \rightarrow 0} \epsilon^{-1} \text{tr} \text{Cov}(\phi)$  is the system's susceptibility, which scales like  $|\text{Re}\lambda_\pm|^{-1}$ , close to the transition. The proof and the general expression is presented in Ref. [40]. Similarly, for the EXP-transition, we find

$$\mathcal{S}^* \propto \chi, \text{ as } \lambda_1 \rightarrow 0, \quad (4)$$

where  $\chi \propto \lambda_1^{-1}$ . Here, the most notable insight is that, in any case, we can identify a component  $\mathbf{J}_0^d \equiv \hat{P}_0 \mathbf{J}^d$ , of the deterministic current pointing in the direction of  $\hat{e}_0$  as the primary source of irreversibility (see Ref. [40] for the precise definition of the projector  $\hat{P}_0$ ). Specifically  $\mathcal{S}^* \sim \lim_{\epsilon \rightarrow 0} \epsilon^{-1} \int_V d\mathbf{r} \langle |\mathbf{J}_0^d|^2 \rangle$ . From Eqs. (3),(4), we conclude that, for both types of transitions,  $\mathcal{S}$  is determined by the inverse of the real part of the eigenvalue that becomes unstable across the transition. Thus, the static phases exhibit, close to the transitions, massively growing (and for  $\epsilon \rightarrow 0$  arbitrarily large) irreversibility, despite their lack of systematic fluxes, and despite their

seemingly equilibrium-like character. Beyond these two transition scenarios, Eq. (2) implies that *any* transition to a dynamical phase with a continuously emerging systematic current is accompanied by a divergence of  $\mathcal{S}^*$  [40].

Within the dynamical phase itself, it follows from Eq. (2) that  $\mathcal{S}$  is of the form

$$\mathcal{S} = \epsilon^{-1} \sum_i \int_V d\mathbf{r} |\nabla^{-1} \partial_t \phi_i^*|^2 + \mathcal{O}(\epsilon^0). \quad (5)$$

The dominant contribution to  $\mathcal{S}$  in the small noise regime is proportional to the integral of the squared local systematic mass current, which is not sensitive to  $\epsilon$ . Thus,  $\mathcal{S}$  diverges in the noise-free limit. If the dynamical phase admits a travelling pattern  $\phi_i^*(\mathbf{r}, t) \equiv \varphi_i(\mathbf{r} - \mathbf{v}t)$ , it follows that  $\mathcal{S} = \epsilon^{-1} |\mathbf{v}|^2 \sum_i \int_V d\mathbf{r} |\varphi_i|^2 + \mathcal{O}(\epsilon^0)$ . The mesoscopic entropy production then signals the emergence of a systematic dissipative mass flux.

*Illustrative Example.*— To illustrate our general findings, we consider a concrete model of type (1), chosen to be as simple as possible while still exhibiting an EXP-transition and an oscillatory instability, namely a stochastic version of the nonreciprocal Cahn-Hilliard model [31–34]. In component form, the dynamical equations for the two-component field  $\phi = (\phi_A, \phi_B)^T$  read

$$\partial_t \phi_A = \nabla \left[ (\alpha + \phi_A^2) \nabla \phi_A - \gamma \nabla^3 \phi_A + (\kappa - \delta) \nabla \phi_B + \sqrt{2\epsilon} \Lambda_A \right], \quad (6a)$$

$$\partial_t \phi_B = \nabla \left[ \beta \nabla \phi_B + (\kappa + \delta) \nabla \phi_A + \sqrt{2\epsilon} \Lambda_B \right]. \quad (6b)$$

The nonreciprocity of the coupling between  $\phi_A$  and  $\phi_B$  is encoded in the parameter  $\delta$ . It ensures that the equations cannot be derived from a scalar potential and represent a non-Hermitian, nonequilibrium model. We study the dynamics on the one-dimensional domain  $[0, 2\pi]$  with periodic boundary conditions. The noise-free ( $\epsilon = 0$ ) case of Eq. (6) was shown to exhibit three distinct phases [31]: a homogeneous phase ( $\phi_{A,B}^* = 0$ ) for small  $\alpha$  and two inhomogeneous “demixed” phases for large  $\alpha$ . The approximate solution in terms of the dominant [31] first Fourier mode  $\phi_{A,B}^{1,*}(r, t) = \mathcal{A}_{A,B}^{1,*} \cos[r + \theta_{A,B}^{1,*}(t)]$  amounts to a static demixed phase for  $\delta < \delta_c = \sqrt{\beta^2 + \kappa^2}$  when  $\partial_t \theta_{A,B}^{1,*}(t) = 0$ , and to a travelling wave phase for  $\delta > \delta_c$  when  $\partial_t \theta_{A,B}^{1,*}(t) = \mathbf{v}$ . The propagation velocity of the travelling wave is  $\mathbf{v} \approx \pm(\delta - \delta_c)^{1/2}$ , with both signs being equally likely. The transition from the homogeneous to the travelling wave state is through an oscillatory instability, while the transition from the static demixed state to the travelling wave state is via an EXP transition. We simulated Eq. (6) using an Euler-Maruyama-algorithm with finite difference gradients, where the domain was discretized by equally spaced mesh points. For a more detailed analytical and numerical investigation of  $\mathcal{S}$  in all

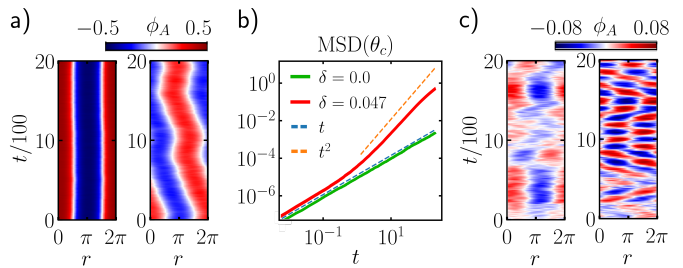


FIG. 2. Dynamics of a fluctuating nonequilibrium Cahn-Hilliard model, Eq. (6), consisting of two nonreciprocally coupled concentration fields  $\phi_A, \phi_B$  for  $\epsilon = 2.5 \times 10^{-5}$  in the static phases. (a) Kymographs of the  $\phi_A$  dynamics in the static demixed phase ( $\alpha = -0.07$ ), *left*: for the reciprocal equilibrium case ( $\delta = 0$ ); *right*: close to the phase transition ( $\delta = 0.92\delta_c = 0.047$ ) and (b) the corresponding MSD of the “center-of-mass” variable  $\theta_c$ . The ballistic regime in the MSD ( $\propto t^2$ ) signals persistent motion of the mean phase and the interfaces; (c) Kymographs of  $\phi_A$  in the mixed phase, close to the phase transition, *left*: for the reciprocal equilibrium case ( $\delta = 0, \alpha = -0.013$ ); *right*: close to the oscillatory instability ( $\delta = 0.06, \alpha = -0.063$ ).

phases and across the transitions, we refer to Ref. [42]. In essence, our analysis confirms our general predictions in Eqs. (3)-(5). In particular, we find a nonzero  $\mathcal{S}$ , which scales like  $\sim \epsilon^0$  in the static (homogeneous and demixed) phases, with singularities of  $\mathcal{S}^*$  at the transitions to the travelling wave phase, and a diverging  $\mathcal{S}^*$  in the travelling wave state itself.

In the remainder, we exploit the explicit model (6) to provide a physical interpretation of our general findings in Eqs. (3)-(5). In particular, we reveal which physical mechanism gives rise to the entropy production (and ultimately its divergence) as the transition is approached.

Let us first consider the dynamical phase itself. The sublinear scaling in  $\epsilon$  [from Eq. (5)] indicates that the dynamical phase exhibits a *macroscopic arrow of time*. Recalling the definition of  $\mathcal{S}$  in terms of path probabilities, a divergent  $\mathcal{S}^*$  means that, upon observation of an (arbitrarily short) realization of the dynamics, one can be 100% sure in which direction time evolves. Where does this certainty come from? The sign of  $\mathbf{v}$  is spontaneously determined by the initial condition and noise only. Thus, the mere propagation of the wave alone *cannot* introduce an arrow of time. However, closer inspection of the solutions of Eq. (6) shows that  $\mathbf{v}$  is aligned with a characteristic phase shift  $\langle \Delta\theta^\pi \rangle \neq 0$ , with  $\Delta\theta^\pi := \theta_A^1 - (\theta_B^1 + \pi)$ . The maxima of  $\phi_B$  always “lag behind” the maxima of  $\phi_A$  as shown in Fig. 1 (b). The alignment of the propagation direction  $\mathbf{v}/|\mathbf{v}|$  with  $\langle \Delta\theta^\pi \rangle$ , which is an apparent manifestation of the  $\mathcal{PT}$  symmetry breaking, introduces the macroscopic arrow of time.

Next, we turn to the static phases and reflect on the manifestation of irreversibility and the reason for the unbounded increase of  $\mathcal{S}^*$  towards the static–dynamic tran-

sition predicted by Eqs. (3), (4). A closer inspection of the  $\phi$  fluctuations in the static demixed phase of Eqs. (6) close to the EXP-transition yields an interesting observation: Namely, the interface dynamics is reminiscent of the irreversible motion of an “active particle” or microswimmer. Formally, this can be seen as follows. As a first step, we recall that the first Fourier mode  $\phi^1$  already encodes the essential information about the transitions [31]. More specifically, it is the phase dynamics  $\theta_{A,B}^1(t)$  that determines the transition from demixed to the travelling wave state. Within the small noise regime, it can (approximately) be separated from higher modes [40], resulting in the closed equations of motion

$$\partial_t \theta^1(t) = \mathbb{A} \cdot \theta^1 + \sqrt{\epsilon/2\pi} \xi, \quad (7)$$

with  $\theta^1 = (\theta_A^1, \tilde{\theta}_B^1)^T$ ,  $\tilde{\theta}_B^1 = \theta_B^1 + \pi$ , and  $\langle \xi_k(t), \xi_l(t') \rangle = (2/\mathcal{A}_k^*)^2 \delta_{k,l} \delta(t-t')$ ,  $k, l \in \{A, B\}$ , and

$$\mathbb{A} = - \begin{pmatrix} \frac{\kappa^2 - \delta^2}{\beta} & -\frac{\kappa^2 - \delta^2}{\beta} \\ -\beta & \beta \end{pmatrix}. \quad (8)$$

One of the eigenvalues of the dynamical operator  $\mathbb{A}$  is strictly zero,  $\lambda_0 = 0$ , reflecting the (native) continuous translational symmetry of the model (6), which is spontaneously broken in the static demixed phase. The other eigenvalue is  $\lambda_1 = -\beta^{-1}(\delta_c^2 - \delta^2)$ . Next, we express the phase dynamics of Eqs. (7),(8) in the “center-of-mass” frame by applying a transformation of the phase coordinates to  $\theta_c := (\Gamma_A \theta_A^1 + \Gamma_B \tilde{\theta}_B^1)/\bar{\Gamma}$  with  $\Gamma_{A,B} := \int_{[0,2\pi]} dr |\phi_{A,B}^{1,*}(r)|^2 = \pi |\mathcal{A}_{A,B}^{1,*}|^2$ ,  $\bar{\Gamma} = \Gamma_A + \Gamma_B$ , yielding

$$\partial_t \theta_c = 2 \underbrace{\frac{\sqrt{\Gamma_A \Gamma_B}}{\bar{\Gamma}} \delta \Delta \theta^\pi}_{=: \mathbf{v}_d} + \sqrt{\frac{2\epsilon}{\bar{\Gamma}}} \xi_c, \quad (9)$$

$$\partial_t \Delta \theta^\pi = \underbrace{-\beta^{-1}(\delta_c^2 - \delta^2)}_{=\lambda_1} \Delta \theta^\pi + \sqrt{\frac{2\epsilon \bar{\Gamma}}{\Gamma_A \Gamma_B}} \xi_\Delta, \quad (10)$$

with  $\langle \xi_\eta(t) \xi_\nu(t') \rangle = \delta_{\eta\nu} \delta(t-t')$ . Equations (9),(10) reveal that for  $|\delta| > 0$ , the “center-of-mass” phase  $\theta_c$  performs a persistent random walk “propelled” by the fluctuating phase shift  $\Delta \theta^\pi$ , in striking analogy to an active swimmer in the Active Ornstein-Uhlenbeck model [43]. The persistence time  $t_p = 1/|\lambda_1|$  and the mean squared propulsion speed  $\langle |\mathbf{v}_d|^2 \rangle = 8\epsilon/(\bar{\Gamma}|\lambda_1|)$  along the swim direction are controlled by the inverse eigenvalue  $\lambda_1^{-1}$  of the dynamical operator  $\mathbb{A}$  in Eq. (8), which vanishes at the transition.

This, in turn, means that the interface between  $\phi_A$  and  $\phi_B$  fluctuates like the path of an active swimmer, which is, by itself indicative of TRSB and accompanying entropy production [44]. Indeed, this is visible in the numerically obtained space-time plots of the full model, see Fig. 2(b). To obtain a quantitative comparison with the interface dynamics of equilibrium demixing,

we use Eq. (9) to compute the mean squared displacement (MSD) of  $\theta_c$  for limits of short and long times and find

$$\text{MSD}(\theta_c) = \begin{cases} \left(t + \frac{1}{2} \frac{\delta^2}{\lambda_1} t^2\right) \frac{\epsilon}{\bar{\Gamma}} & t \ll t_p \\ \left(1 + \frac{\delta^2}{\lambda_1}\right) t \frac{\epsilon}{\bar{\Gamma}} & t \gg t_p. \end{cases} \quad (11)$$

Clearly, the “activity” for  $|\delta| > 0$  is revealed by a ballistic intermediate asymptotic regime and a strongly enhanced late-time diffusion coefficient in the vicinity of the transition ( $\lambda_1 \rightarrow 0$ ). The predictions of our approximate solution are nicely confirmed by the numerical data presented in Fig. 2(a) showing the MSD of the interface dynamics obtained directly from Eq. (6). The “active fluctuations” of the interface dynamics represent a concrete manifestation of TRSB on timescales comparable to the persistence time; in the same manner as it does for an active swimmer (note that here, both variables are even under time-reversal [45]). As can immediately be gleaned from Eq. (9), this TRSB yields a considerable fraction  $\mathcal{S}_{\theta_c}^* < \mathcal{S}^*$  of the total entropy production. It is generated by the irreversible mesoscopic current of intensity  $\mathbf{v}_d$  pointing in the direction of the Goldstone mode, where  $\mathcal{S}_{\theta_c}^* = \bar{\Gamma} \langle |\mathbf{v}_d|^2 \rangle$ . For our example, it originates from the dissipative mass flux of the coherent motion of both fields, represented by  $\theta_c$ . As the transition to the dynamical phase is approached ( $\delta \rightarrow \delta_c$ ), the “propulsion speed” and its associated persistence time increase unboundedly, resulting in an unbounded increase of  $\mathcal{S}^*$ . Importantly, the persistent motion of  $\theta_c$  in Eq. (9) is always oriented *towards* the phase shift  $\Delta \theta^\pi$  (which has zero mean,  $\langle \Delta \theta^\pi \rangle = 0$ , contrasting the  $\mathcal{PT}$ -broken travelling wave state), see Fig. 1(b). Such unidirectional coupling between the damped modes (here  $\Delta \theta^\pi$ ) and a Goldstone mode (here  $\theta_c$ ) that does not vanish at the transition is a hallmark of EXP transitions and only possible for non-Hermitian dynamical operators. On the one hand, this generically leads to a conversion and amplification of fluctuations into the direction of the Goldstone mode. As was recently described in the context of quantum system [46] and as we discuss for general field models of type (6) in Ref. [40], this very mechanism is deeply connected with the origin of  $\mathcal{PT}$ -symmetry breaking at the EXP transition. On the other hand, the unidirectional coupling can be understood as a most extreme violation of detailed balance.

Lastly, also for the divergence of  $\mathcal{S}^*$  at the oscillatory instability, the nonreciprocal Cahn-Hilliard model provides a rather intuitive interpretation. Noting that  $|\text{Im}\lambda_\pm|$  corresponds to the frequency of the limit cycle, we find that  $\mathcal{S}$  signals the presence of cyclic currents in the homogeneous phase. Their amplitude is entirely due to transient fluctuations, but eventually becomes systematically positive as  $\chi$  diverges at the transition. In our example this mechanism results in the form of temporarily stable travelling waves, which are plainly obvious in

the graphical representation of our simulation data, see Fig. 2(c).

*Conclusions.*— We have studied the irreversibility of the fluctuations of coarse-grained hydrodynamic field models close to the onset of dynamical phases. Clearly, the dynamical phase itself is a particularly drastic manifestation of TRSB, but our results show that even before a system enters this state, it already reveals its nonequilibrium character through “irreversible” TRSB fluctuations around a seemingly equilibrium-like average behavior. This observation could be of interest for a nonequilibrium classification of living matter [12]. Focusing on two paradigmatic transition scenarios, we found that the formation of dynamical phases is accompanied by a divergence of the entropy production rate  $\mathcal{S}$  in the zero-noise limit. The effect is indeed indicative of any continuous static–dynamic phase transition scenario. The fluctuating dynamics becomes increasingly irreversible as one approaches the dynamical phase, attaining a deterministic character at the transition. In the small noise regime,  $\mathcal{S}$  scales just as the susceptibility, or equivalently, as the inverse of the characteristic eigenvalue that becomes unstable across the transition. Moreover, we have drawn general connections between the  $\mathcal{PT}$ -symmetry breaking and TRSB of the fluctuations, at an exceptional point. We were able to attribute the striking simultaneous presence of two completely different forms of symmetry breaking ( $\mathcal{PT}$  and TRSB) to a common origin, a nonequilibrium conversion of thermal into irreversible fluctuations. Our analysis of a model consisting of two nonreciprocally coupled, noisy Cahn-Hilliard fields confirmed our general findings and provided instructive physical interpretations for the TRSB in terms of a peculiar phenomenology of “active interface dynamics”. In future studies, it would be interesting to reconsider our findings from the perspective of “information thermodynamics” as recently pioneered for Turing patterns [47]. Finally, concerning extensions of our analysis towards discontinuous transitions such as those observed in Refs. [8, 48], one may suspect that a very different picture could emerge.

This work was funded by the Deutsche Forschungsgemeinschaft (DFG, German Research Foundation) through the project 498288081. We thank Étienne Fodor and Jeremy O’Byrne for valuable comments.

---

\* sl2127@cam.ac.uk

- [1] A. Einstein and M. Klein, The collected papers of Albert Einstein: The Swiss years: Correspondence, 1902-1914 (Princeton University Press, 1993) p. 44.
- [2] R. Hooke, The posthumous works of Robert Hooke (Routledge, 2019) p. 116.
- [3] U. Seifert, Entropy production along a stochastic trajectory and an integral fluctuation theorem, *Phys. Rev. Lett.* **95**, 040602 (2005).
- [4] É. Roldán and J. M. R. Parrondo, Entropy production and Kullback-Leibler divergence between stationary trajectories of discrete systems, *Phys. Rev. E* **85** (2012).
- [5] Y. I. Li and M. E. Cates, Steady state entropy production rate for scalar Langevin field theories, *J. Stat. Mech. Theory Exp.* **2021**, 013211 (2021).
- [6] C. Nardini, E. Fodor, E. Tjhung, F. van Wijland, J. Tailleur, and M. E. Cates, Entropy production in field theories without time-reversal symmetry: Quantifying the non-equilibrium character of active matter, *Phys. Rev. X* **7**, 021007 (2017).
- [7] D. S. Seara, B. B. Machta, and M. P. Murrell, Irreversibility in dynamical phases and transitions, *Nat. Commun.* **12**, 1 (2021).
- [8] Ø. Borthne, E. Fodor, and M. Cates, Time-reversal symmetry violations and entropy production in field theories of polar active matter, *New J. Phys.* **22**, 123012 (2020).
- [9] G. Pruessner and R. Garcia-Millan, Field theories of active particle systems and their entropy production (2022).
- [10] S. Ro, B. Guo, A. Shih, T. V. Phan, R. H. Austin, D. Levine, P. M. Chaikin, and S. Martiniani, Model-free measurement of local entropy production and extractable work in active matter, *Phys. Rev. Lett.* **129**, 220601 (2022).
- [11] T. H. Tan, G. A. Watson, Y.-C. Chao, J. Li, T. R. Gingrich, J. M. Horowitz, and N. Fakhri, Scale-dependent irreversibility in living matter, arXiv preprint arXiv:2107.05701 (2021).
- [12] C. Battle, C. P. Broedersz, N. Fakhri, V. F. Geyer, J. Howard, C. F. Schmidt, and F. C. MacKintosh, Broken detailed balance at mesoscopic scales in active biological systems, *Science* **352**, 604 (2016).
- [13] M. Bestehorn, R. Friedrich, and H. Haken, Traveling waves in nonequilibrium systems, *Phys. D: Nonlinear Phenom.* **37**, 295 (1989).
- [14] M. Bestehorn, R. Friedrich, and H. Haken, Two-dimensional traveling wave patterns in nonequilibrium systems, *Z. Phys. B.* **75**, 265 (1989).
- [15] S. Ghosh, S. Gutti, and D. Chaudhuri, Pattern formation, localized and running pulsation on active spherical membranes, *Soft Matter* **17**, 10614 (2021).
- [16] S. Ramaswamy, J. Toner, and J. Prost, Nonequilibrium fluctuations, traveling waves, and instabilities in active membranes, *Phys. Rev. Lett.* **84**, 3494 (2000).
- [17] M. Agrawal, I. R. Bruss, and S. C. Glotzer, Tunable emergent structures and traveling waves in mixtures of passive and contact-triggered-active particles, *Soft Matter* **13**, 6332 (2017).
- [18] E. Frey, J. Halatek, S. Kretschmer, and P. Schwille, Protein pattern formation, in *Physics of biological membranes* (Springer, 2018) pp. 229–260.
- [19] K. C. Huang, Y. Meir, and N. S. Wingreen, Dynamic structures in Escherichia coli: spontaneous formation of Mine rings and Mind polar zones, *Proc. Natl. Acad. Sci. U. S. A.* **100**, 12724 (2003).
- [20] S.-i. Amari, Dynamic of pattern formation in lateral-inhibition type neural fields, *Biol. Cybern.* **27**, 77 (1977).
- [21] J. Wang, Landscape and flux theory of non-equilibrium dynamical systems with application to biology, *Adv. Phys.* **64**, 1 (2015).
- [22] S. Bhattacharya, T. Banerjee, Y. Miao, H. Zhan, P. Devreotes, and P. Iglesias, Traveling and standing waves mediate pattern formation in cellular protrusions, *Sci.*

- Adv. **6**, eaay7682 (2020).
- [23] R. Welch and D. Kaiser, Cell behavior in traveling wave patterns of myxobacteria, *Proc. Natl. Acad. Sci. U. S. A.* **98**, 14907 (2002).
- [24] S. Takada, N. Yoshinaga, N. Doi, and K. Fujiwara, Mode selection mechanism in traveling and standing waves revealed by min wave reconstituted in artificial cells, *Sci. Adv.* **8**, eabm8460 (2022).
- [25] A. Goldbeter, Dissipative structures in biological systems: bistability, oscillations, spatial patterns and waves, *Philos. Trans. R. Soc. A* **376**, 20170376 (2018).
- [26] M. C. Cross and P. C. Hohenberg, Pattern formation outside of equilibrium, *Rev. Mod. Phys.* **65**, 851 (1993).
- [27] E. Tiezzi, R. Pulselli, N. Marchettini, and E. Tiezzi, Dissipative structures in nature and human systems (2008) pp. 293–299.
- [28] B. N. Belintsev, Dissipative structures and the problem of biological pattern formation, *Sov. phys., Usp.* **26**, 775 (1983).
- [29] G. Gambino, M. Lombardo, and M. Sammartino, Turing instability and pattern formation for the Lengyel-Epstein system with nonlinear diffusion, *Acta Appl. Math.* **132** (2014).
- [30] M. Fruchart, R. Hanai, P. B. Littlewood, and V. Vitelli, Non-reciprocal phase transitions, *Nature* **592**, 363369 (2021).
- [31] Z. You, A. Baskaran, and M. C. Marchetti, Nonreciprocity as a generic route to traveling states, *Proc. Natl. Acad. Sci. U. S. A.* **117**, 1976719772 (2020).
- [32] S. Saha, J. Agudo-Canalejo, and R. Golestanian, Scalar active mixtures: The nonreciprocal Cahn-Hilliard model, *Phys. Rev. X* **10** (2020).
- [33] T. Frohoff-Hülsmann, J. Wrembel, and U. Thiele, Suppression of coarsening and emergence of oscillatory behavior in a Cahn-Hilliard model with nonvariational coupling, *Phys. Rev. E* **103**, 042602 (2021).
- [34] T. Frohoff-Hülsmann and U. Thiele, Nonreciprocal cahn-hilliard equations emerging as one of eight universal amplitude equations, arXiv preprint arXiv:2301.05568 (2023).
- [35] R. Mandal, S. S. Jaramillo, and P. Sollich, Robustness of travelling states in generic non-reciprocal mixtures (2022).
- [36] R. Kubo, The fluctuation-dissipation theorem, *Rep. Prog. Phys.* **29**, 255 (1966).
- [37] P. Coullet, R. E. Goldstein, and G. H. Gunaratne, Parity-breaking transitions of modulated patterns in hydrodynamic systems, *Phys. Rev. Lett.* **63**, 1954 (1989).
- [38] H. Z. Cummins, L. Fourtune, and M. Rabaud, Successive bifurcations in directional viscous fingering, *Phys. Rev. E* **47**, 1727 (1993).
- [39] L. Pan and J. R. de Bruyn, Spatially uniform traveling cellular patterns at a driven interface, *Phys. Rev. E* **49**, 483 (1994).
- [40] Supplemental Material.
- [41] Y. Ashida, Z. Gong, and M. Ueda, Non-hermitian physics, *Adv. Phys.* **69**, 249435 (2020).
- [42] In preparation.
- [43] L. Caprini, U. M. B. Marconi, A. Puglisi, and A. Vulpiani, The entropy production of ornstein–uhlenbeck active particles: a path integral method for correlations, *J. Stat. Mech. Theory Exp.* **2019**, 053203 (2019).
- [44] G. Falasco, R. Pfaller, A. P. Bregulla, F. Cichos, and K. Kroy, Exact symmetries in the velocity fluctuations of a hot brownian swimmer, *Phys. Rev. E* **94**, 030602 (2016).
- [45] S. Shankar and M. C. Marchetti, Hidden entropy production and work fluctuations in an ideal active gas, *Phys. Rev. E* **98**, 020604 (2018).
- [46] R. Hanai and P. B. Littlewood, Critical fluctuations at a many-body exceptional point, *Phys. rev. res.* **2** (2020).
- [47] G. Falasco, R. Rao, and M. Esposito, Information thermodynamics of Turing patterns, *Phys. Rev. Lett.* **121**, 108301 (2018).
- [48] T. Agranov, S. Ro, Y. Kafri, and V. Lecomte, Macroscopic fluctuation theory and current fluctuations in active lattice gases (2022).